Polymer 195 (2020) 122454

Contents lists available at ScienceDirect

Polymer

journal homepage: http://www.elsevier.com/locate/polymer

Systematic evaluation of cyanate ester/ epoxidized cresol novolac copolymer resin system for high temperature power electronic packaging applications

Jiaxiong Li [a,1], Chao Ren [b,1], Dong An [c], Yanjuan Ren [d], Kyoung-sik Moon [a], Ching-ping Wong [a,*]

[a] School of Materials Science and Engineering, Georgia Institute of Technology, Atlanta, GA, 30332, United States
[b] School of Biological and Chemical Engineering, Anhui Polytechnic University, Wuhu, Anhui, 241000, China
[c] Shanxi Key Laboratory of Nano-functional Composite Materials, North University of China, Taiyuan, Shanxi, 030051, China
[d] Department of Materials Science and Engineering, CAPT/ HEDPS/LTCS, Key Laboratory of Polymer Chemistry and Physics of Ministry of Education, College of Engineering, Peking University, Beijing, 100871, China

ARTICLE INFO

Keywords:
Epoxy molding compound
Cyanate ester
Thermal degradation

ABSTRACT

The power electronics industry has been actively seeking high temperature stable epoxy molding compound (EMC) materials that can meet the requirements for encapsulating future SiC chips operating at a temperature (250 °C) that exceeds the capability of current epoxy chemistry. This work provides a detailed evaluation of a high heat resistant cyanate ester (CE)/epoxidized cresol novolac (ECN) copolymer system with varied compositions regarding their high temperature performances. Owing to the novolac nature of ECN which provides a high crosslink density, it is found that the copolymers with a low CE concentration (25–33 mol%) are able to produce a comparable glass transition temperature (>230 °C) and decomposition temperature ($T_{10\%}$>400 °C) to those of the high CE formulations. Moreover, long-term high temperature (250 °C) storage test of reveals a less severe weight loss and blistering in the lower CE formulations. A distinguished degradation mechanism involving hydrolysis of unreacted cyanate groups in the high CE compositions was determined through various thermal and chemical analyses. It was concluded that the CE/ECN copolymers with low CE concentrations are promising candidates for the high temperature EMC formulation.

1. Introduction

Epoxy molding compound (EMC) has been the standard encapsulation technology in electronic packaging industry to protect the electronic system from external stress and moistures. The use of epoxy (EP) resin and silica filler provides the compound a good overall performance including adhesion strength, chemical resistance and mechanical robustness [1,2]. Recently, the power electronics industry has been craving novel encapsulant materials that can serve in harsher environments for various consumer, power and automotive applications [3,4]. In fact, the thermal stability of the encapsulant material has become a bottle neck for further adopting high performance SiC chips in the molded power cards [5–8].

Novolac type EP resin including EPN (epoxidized phenol novolac) resin or ECN (epoxidized cresol novolac) resin cured with the phenolic resin is widely used in EMC industry for high temperature encapsulations, owing to their high aromaticity and high functionality nature [9,10]. However, the difficulty in achieving T_g over 200 °C still remains and the long-term aging behavior is far from satisfaction [11–13]. Blending of other thermally stable resins into EP has been an actively reported approach in the past decades, which include polyimide [14], bismaleimide (BMI) [15], cyanate ester (CE) [16–18], phthalonitrile [19], benzocyclobutene (BCB) [20] etc. Despite their enhanced high temperature performance, most of those high temperature resins however suffer from the high cost, high curing temperature and the brittleness, the latter due to their highly crosslinked networks [15]. Of these high temperature polymers, the CE resin is a promising candidate for high temperature encapsulant application due to its balanced thermal and mechanical performance, attracting dielectric properties and moreover, the good compatibility with EP chemistry [21,22]. The curing

* Corresponding author.
E-mail address: cp.wong@mse.gatech.edu (C.-p. Wong).
[1] These two authors contributed equally to this work.

https://doi.org/10.1016/j.polymer.2020.122454
Received 15 November 2019; Received in revised form 31 March 2020; Accepted 3 April 2020
Available online 8 April 2020
0032-3861/© 2020 Elsevier Ltd. All rights reserved.

Table 1
An example of CE/ECN copolymer blend formulation calculated from the ratio between cyanate groups and epoxide groups. The Cu (II) catalyst dosages were determined by their concentrations to the CE parts.

CE/ECN (cyanate: epoxide)	CE/g	ECN/g	Cu(II) acac/g
1:3	1.0	4.2	0.0315
1:2	1.0	2.8	0.0315
1:1	1.0	1.4	0.0315
2:1	1.0	0.7	0.0315
3:1	1.0	0.5	0.0315

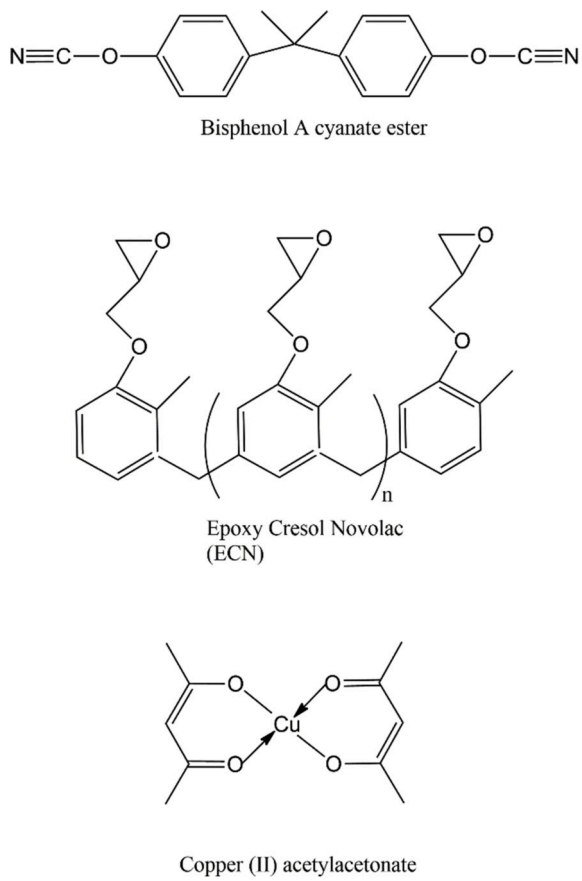

Fig. 1. Chemical structure of CE, ECN and Cu (II) acac.

of CE multifunctional monomer makes use of the trimerization of cyanate functional groups to form *s*-triazine structure and crosslink, and this increase of aromaticity produces the superior high temperature properties of cured resin.

One of the earliest inventions that produced commercially significant product utilizing CE/EP copolymer chemistry is the bismaleimide/triazine (BT) resin introduced by Mitsubishi Gas Chemical Company that is widely used in substrate applications [23]. However, the BT products in the early days suffered from severe blistering due to the impure CE monomers. More significant reports on the CE/EP copolymers with much improved performance could be found the later developments in late 80s and early 90s by Shimp, Ising and Christenson [21,24]. J. Bauer and M. Bauer [25–27] have conducted extensive researches in the field of curing chemistry and kinetics of CE/EP co-reactions and provided fundamental understandings into the multi-step reaction mechanism which was verified by Hamerton et al. [28]. Later on, Kim [29] reported the effects of CE on facilitating curing and enhancing the thermal stability of a bisphenol A EP. Lin [30] studied the curing reaction in two kinds of CE/EP blends and proposed different reaction pathways in bisphenol A type and cycloaliphatic type EP systems. Su and Chuang

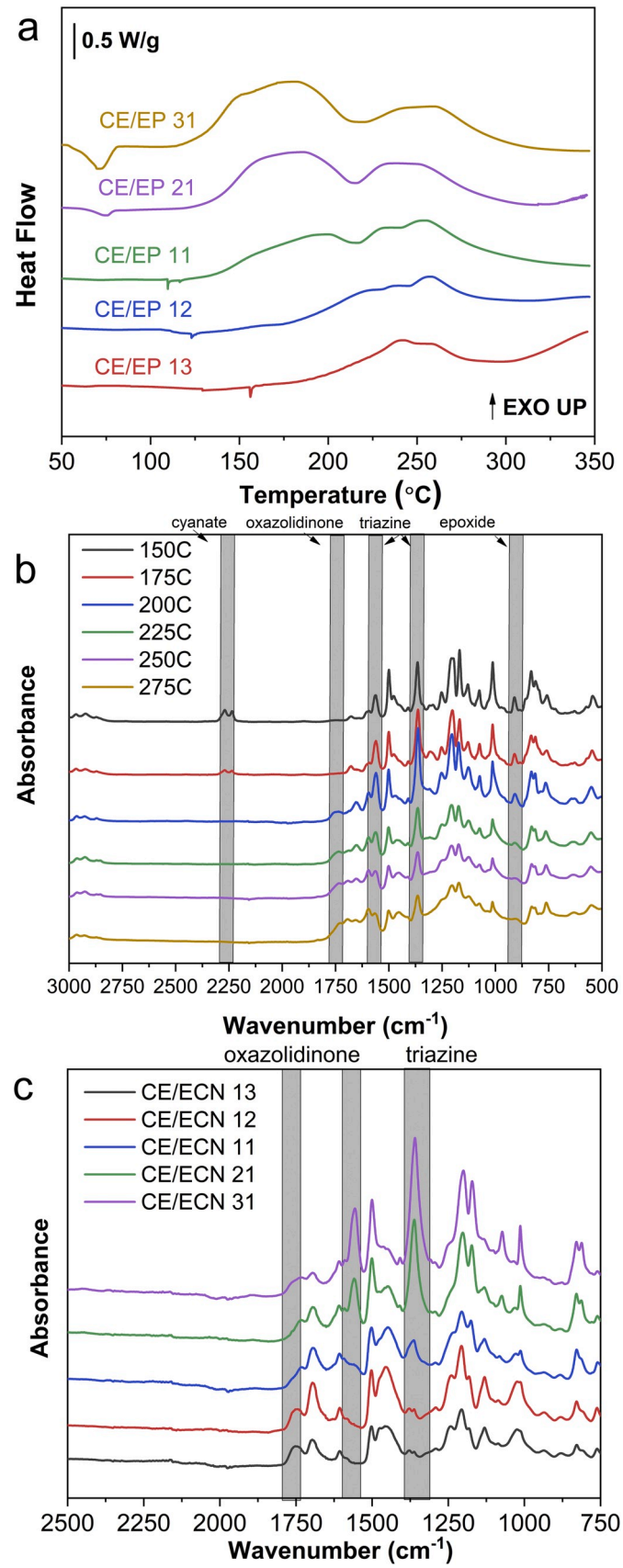

Fig. 2. (a) DSC curing profiles of the CE/ECN blends at different ratios; (b) FTIR spectra of CE/ECN blends at 1: 1 M ratio during temperature ramp; (c) FTIR spectra of CE/ECN blends with different feed ratios.

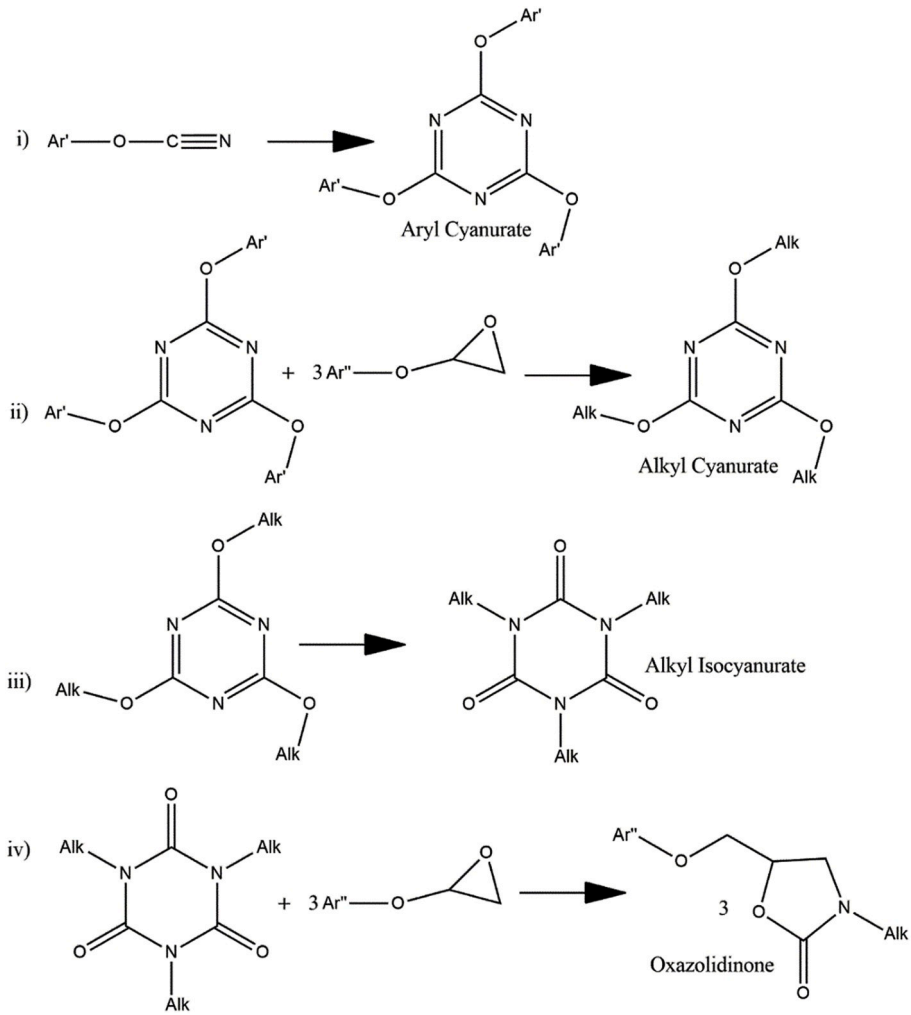

Fig. 3. Chemical reactions involved in the CE/EP copolymer curing proposed by Shimp [37].

Table 2
Results from TMA tests on CE/ECN blends including the T_g and CTE before and after glass transition.

CE/ECN	TMA T_g/°C	α_1/ppm/°C	α_2/ppm/°C
1:3	203.5	67.2	228.7
1:2	222.0	64.6	216.7
1:1	235.8	61.0	160.1
2:1	237.9	58.3	253.8
3:1	248.9	60.4	279.7
CE	261.7	86.1	210.2

[31] demonstrated the different tendency of the triazine and oxazolidinone formation in the ortho-substituted EP and CE blends where triazine formation is encouraged due to the steric hindrance. Ren et al. [32] described the introducing of EP in commercial CE to improve both mechanical strength and moisture absorption behavior. Lei et al. [33] studied the curing reaction in imidazole catalyzed CE/EP blends and proposed the reaction route for the two different stage of curing in the copolymer blend. Quite recently, the works in Hamerton group [34,35] regarding the thermal and mechanical properties of several CE/EP blends based on CE monomers carrying different structural units have demonstrated excellent thermal stability of the copolymer blends and revealed the direct relationship between crosslinked network structure and thermal degradation parameters. For the high temperature encapsulant applications, the CE/EP copolymer system using bisphenol A type CE and biphenyl type EP has previously been characterized by our group [36]. Although a higher T_g and thermal decomposition temperature were found when increasing the CE content, the long-term high temperature aging test showed reversed results. A higher CE concentration in the copolymer system led to a larger weight loss during aging with the early failure with blistering and cracking of the sample. Further studies are still needed for exploring high performance copolymers with balanced thermal properties to fulfill the requirements for future high-power electronics packaging.

In this work, an ECN type EP was selected to formulate high heat resistant CE/ECN copolymer resins. A systematic evaluation of the copolymer properties with different resin compositions was performed. The curing reaction and its chemistry were investigated with differential scanning calorimeter (DSC) and Fourier transformation infra-red (FTIR) spectroscopy. The thermo-mechanical properties of the resins revealed interesting material characteristics, where the low CE formulations exhibited competitive performance and that was attributed to their high functionality nature. Moreover, high temperature storage tests were performed on the copolymer samples to evaluate the reliability of the molding material subjected to device working condition (250 °C). The effects of aging on sample weight, thermal expansions, chemical structures and decomposition profiles were characterized, where a distinguished degradation pattern of the high CE formulations due to stress induced by the outgas from carbamate decomposition that related to the hydrolysis of cyanate groups are discussed. The copolymers with 25 mol % to 33 mol % CE feed ratios are determined to be the best formulations and stand out as very promising candidates for future studies towards

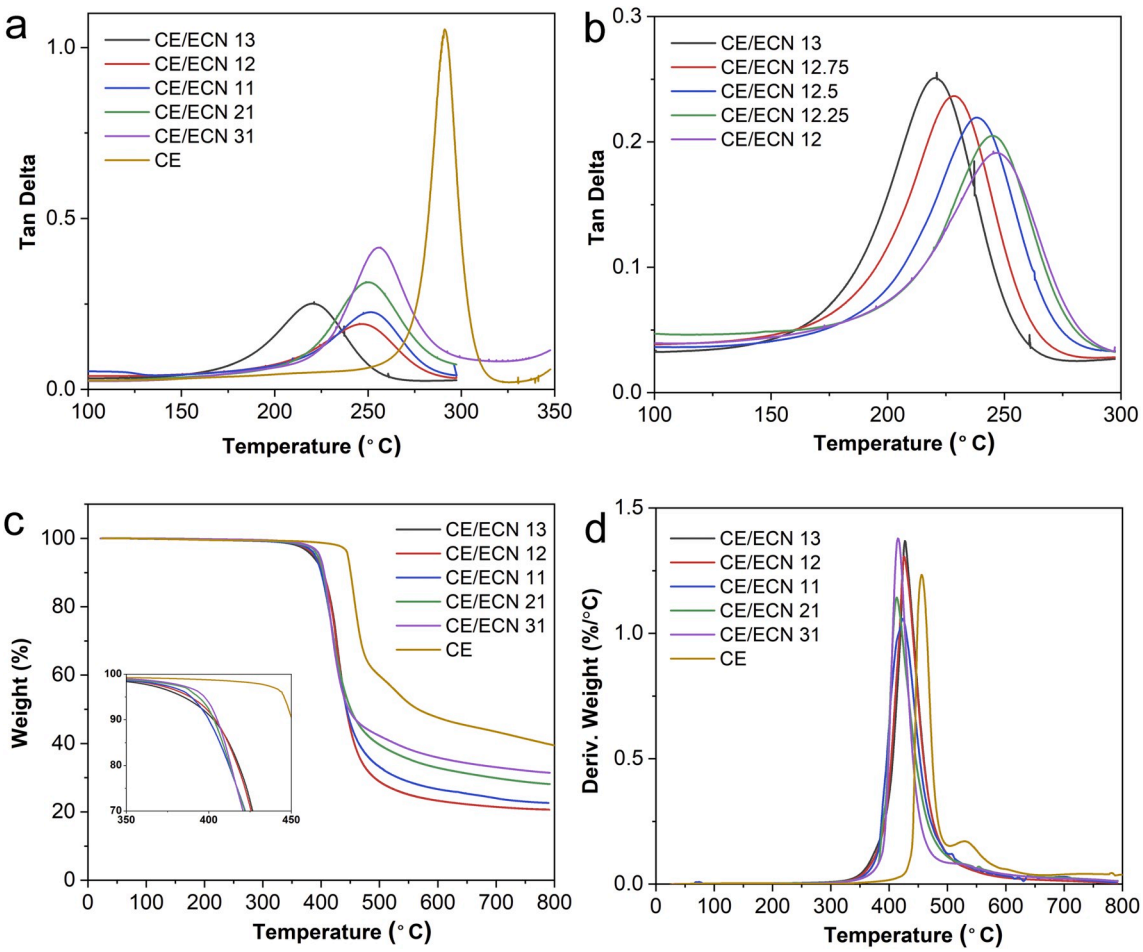

Fig. 4. (a) DMA tan δ profiles of CE/ECN blends ranging from 1:3 to 3:1 and pure CE; (b) DMA tan δ profiles of CE/ECN blends from 1:3 to 1:2; (c) TGA weight loss diagram of CE/ECN blends in N_2. The inset magnifies the 350 °C- 450 °C region.; (d) DTG diagram of CE/ECN blends.

Table 3
DMA results of the CE/ECN blends.

CE/ECN	DMA T_g/°C	G′ at 30 °C above T_g/MPa	Crosslink density/10^{-3} mol/cm^3
1:3	221.1	114.5	18.3
1:2.75	228.6	129.8	20.1
1:2.5	238.5	134.0	20.0
1:2.25	245.3	154.0	22.4
1:2	247.6	133.1	19.2
1:1	251.7	130.5	18.6
2:1	248.9	115.7	16.6
3:1	256.7	61.3	8.6
CE	291.1	19.0	2.4

Table 4
Summarized parameters from TGA and DTG profiles of the CE/ECN blends.

CE/ECN	$T_{5\%}$ in N_2/°C	$T_{10\%}$ in N_2/°C	Char Yield at 800 °C/%	T_i/°C	T_p/°C
1:3	384.7	403.1	20.7	393.2	427.2
1:2	389.0	404.1	20.7	390.4	425.8
1:1	389.5	400.2	22.6	381.1	423.0
2:1	393.8	403.2	28.1	390.2	412.9
3:1	397.5	405.2	31.5	392.2	415.2
CE	445.4	450.5	39.4	439.7	455.8

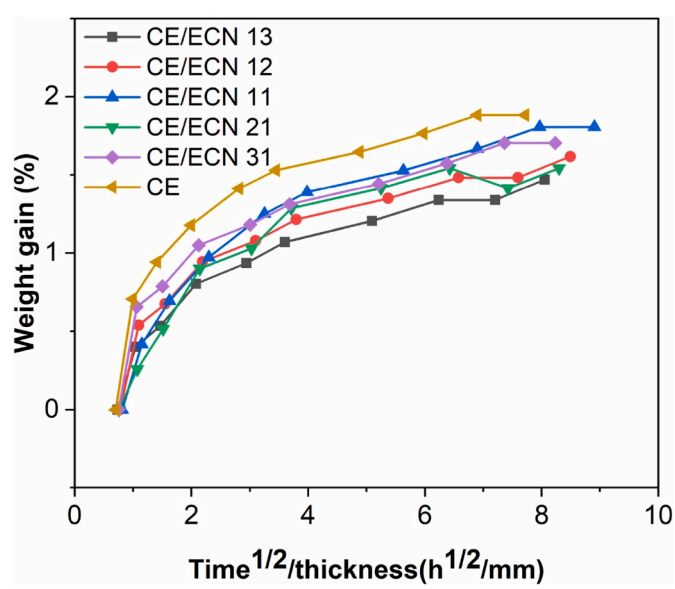

Fig. 5. Moisture absorption of CE/ECN blends under 85 °C/85 RH condition.

Table 5
Dielectric constant and loss factor of CE/ECN blends at 10 MHz.

CE/ECN	D_k @ 10 MHz	D_f @ 10 MHz
13	3.25	0.023
12	3.33	0.020
11	3.11	0.022
21	3.08	0.026
31	2.95	0.017

high temperature EMC applications.

2. Materials and characterization

ESCN 195XL resin (ECN) was obtained from Sumitomo Chemical, Tokyo, Japan, with an epoxide equivalent weight (E.E.W.) of 195. 2,2-bis(4-cyanatophenyl)propane (CE, CAS# 1156-51-0, 96%) was purchased from Oakwood Chemical, Estill, USA. Copper (II) acetylacetonate (Cu (II) acac, CAS# 13395-16-9, 99.99+%) and nonylphenol (CAS# 84852-15-3, technical grade) were purchased from Aldrich. The reagents were used as received. All the polymer blends were based on the molar ratio between cyanate groups from CE and epoxide groups (i.e. CE/ECN 13 represents formulation with cyanate: epoxide of 1:3 M ratio). In this work, five different CE/ECN copolymer compositions ranging from 1:3 M ratio to 3:1 M ratio (namely 1:3, 1:2, 1:1, 2:1 and 3:1) were under investigation. Acetone (CAS# 67-64-1, ≥99.5%, ACS grade) was used for dissolving the CE and ECN monomers assisted by sonication at 50% amplitude for 30 min (Q700 Sonicator, Qsonica, Newton, USA). The catalyst Cu (II) acac and co-catalyst nonylphenol were pre-mixed at desired ratio and added drop wise into the CE/ECN acetone solution at a concentration of 360 ppm of Cu (II) ion and 3 phr of nonylphenol to the CE resin. An example of the detailed monomer feed weights in each formulation calculated form the abovementioned methodology is given in Table 1. The well-mixed solution was casted in to aluminum weighing pan (28 mm diameter) and later placed in a vacuum oven to remove all the solvents before curing. Curing schedule of the samples were 2 h at 150 °C, 2 h at 200 °C and 3 h at 250 °C with ramping rate of 10 °C/min. Final cured disk-shaped samples were polished for aging tests and cut into desired dimensions for thermo-mechanical tests. The chemical structure of the CE, ECN and the catalyst used are shown in Fig. 1.

Differential scanning calorimetry (DSC) was done by ramping at 10 °C/min from 40 °C to 350 °C under 50 mL/min nitrogen flow (DSC Q2000, TA Instrument, New Castle, USA). In each scanning, approximately 10 mg of sample was encapsulated in the aluminum sealed pans without piercing. Thermal mechanical analysis (TMA) was ramped at 20 °C/min from 40 °C to 300 °C under 50 mL/min nitrogen flow (TMA Q400, TA Instrument, New Castle, USA) with expansion probe. The TMA samples were made by cutting the cured resins to 10 mm × 10 mm × 1 mm size. Dynamic mechanical analysis (DMA) was performed in tension mode with film dimension at 10 mm × 8 mm × 1 mm, ramped at 3 °C/min from 40 °C to 300 °C in air atmosphere at oscillation frequency of 1 Hz (DMA Q800, TA Instrument, New Castle, USA). The thermal gravimetric analysis (TGA) tests were programmed to ramp 20 °C/min from 40 °C to 800 °C under 50 mL/min nitrogen flow (TGA Q50, TA Instrument, New Castle, USA) using approximately 10 mg of sample in the platinum Q50 pans. The disk-shaped samples with 28 mm diameter and approximately 1 mm thickness were used in all the following tests. Dielectric permittivity and loss of the samples were scanned from 1 MHz to 1 GHz (E4991A RF Impedance Analyzer, Agilent, Santa Clara, USA) at room temperature. Fourier-transform infrared spectroscopy (FTIR) was performed using diamond attenuated total reflectance (ATR) mode (Nicolet iS5 FT-IR spectrometer, Thermo Scientific, Waltham, USA) with resolution of 4 cm^{-1} from 500 cm^{-1} to 3500 cm^{-1}, 64 scans were done for each sample. An in-situ FTIR measurement to track down the sample chemical structure evolutions during cure was carried out on samples quenched at a desired temperature from a temperature ramp with 10 °C/min. The moisture absorption measurement was done at 85 °C/85 relative humidity (RH) atmosphere (MicroClimate bench top environmental chamber, Cincinnati SubZero Inc., Cincinnati, USA) and taken out at different time intervals to measure weight gain. The high temperature aging test was performed at 250 °C in circulating air (825f convection oven, Fisher Scientific, USA, Waltham, USA) where weight loss, chemical structure and thermo-mechanical properties of the samples over aging time were recorded as well as the chemical structure change.

Table 6
Parameters from TMA tests on CE/ECN blends during aging under 250 °C aging including the T_g and CTE before and after glass transition.

CE/ECN	Aging time/h	TMA T_g/°C	α_1/ppm/°C	α_2/ppm/°C
1:3	0	203.5	67.2	228.7
	4	237.5	77.7	192.3
	8	226.6	75.7	198.0
	24	201.4	66.0	247.2
	48	200.6	75.1	489.5
1:1	0	235.8	61.0	160.1
	4	238.3	79.7	234.4
	8	203.7	65.4	251.3
	24	202.5	71.0	344.5
	48	161.3	65.8	290.1
3:1	0	248.9	60.4	279.7
	4	239.0	59.5	303.5
	8	210.5	51.8	295.6
	24	189.6	68.5	224.3
	48	173.2	97.2	275.7

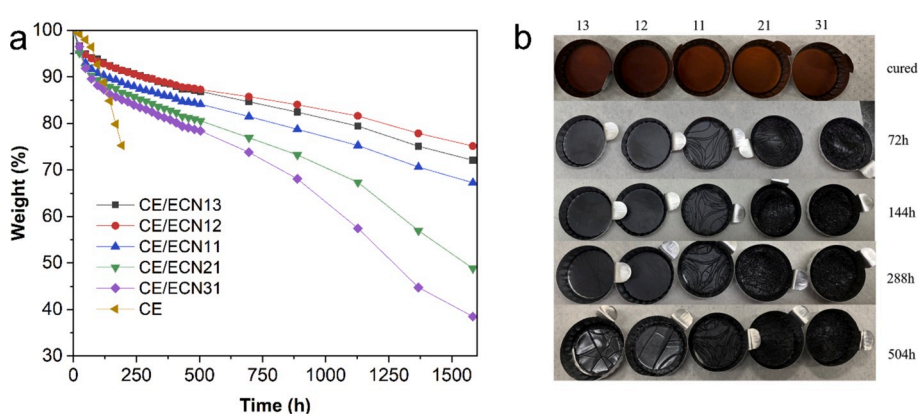

Fig. 6. (a) Weight change of CE/ECN blends under 250 °C aging; (b) Pictures of CE/ECN blends under 250 °C aging for different period of time. The number on top denotes the formulation of the copolymer.

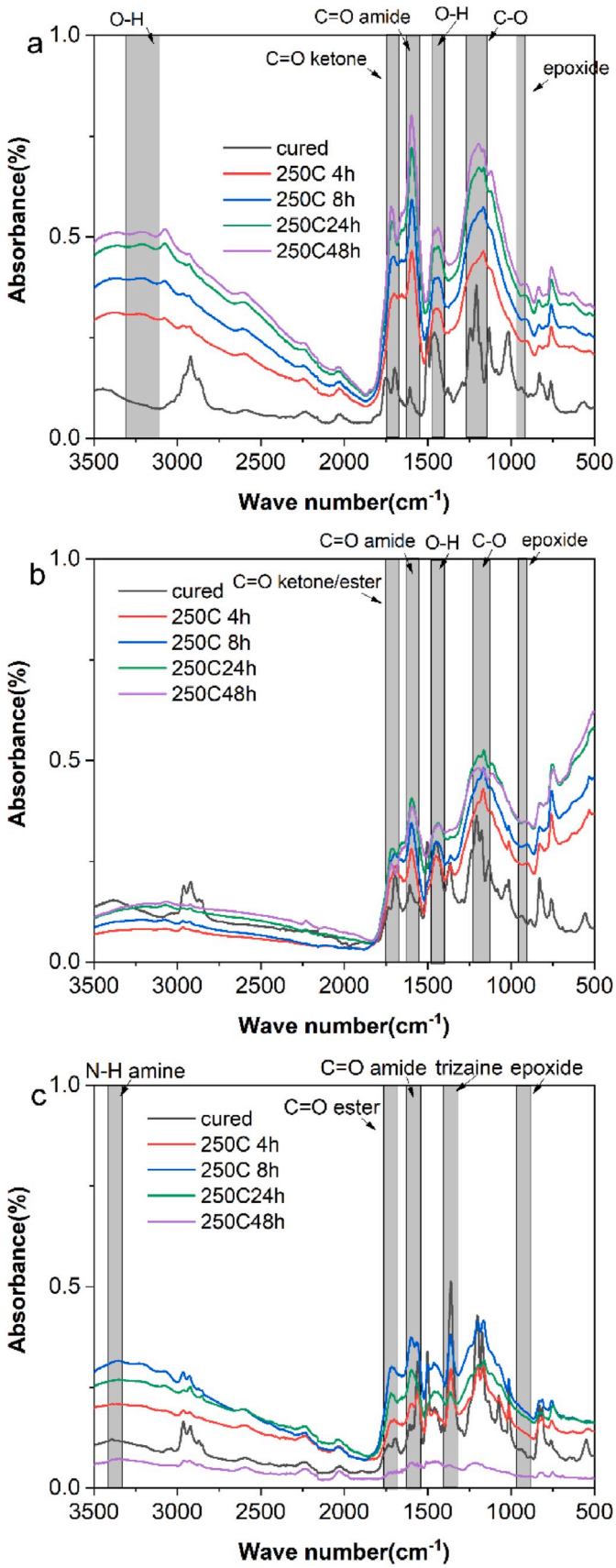

Fig. 7. FTIR spectra of (a) CE/ECN 1:3 blend, (b) CE/ECN 1:1 blend and (c) CE/ECN 3:1 blend during 250 °C aging.

3. Results and discussion

The curing profiles of the CE/ECN copolymer formulations were monitored by DSC scans and are shown in Fig. 2(a). The exothermic peaks of these copolymers are rather complicated, possibly due to the side reactions in the system from the presence of unepoxidized hydroxyl groups in the ECN. However, general rules could be found in these profiles. In high CE content blends, the curing exotherms can be divided into two regions, one with the peak temperature around 150 °C and the other at 250 °C. The area under the first exothermic peak decreases and the second one increases with lowering CE feed ratios, and it is also noted that the lower CE concentration copolymers generated a less amount of exothermic heat during the curing reaction.

It is proposed here the origin of these two major peaks represent different stages of reactions in the CE/EP co-curing chemistry (see Fig. 3), which is clarified in the previous works down by Bauer et al. [38], indicating the temperature preferences of different reactions. The co-curing of CE an EP resin would involve several steps of chemical reactions, namely the formation of triazine ring, the epoxide insertion on triazine ring, reformation of isocyanurate rings and the subsequent ring cleavage and its reaction with epoxides to form oxazolidinone. In this sense, seemly contradictory to the common knowledge of binary copolymer systems based on step-growth mechanism, even when the monomers feed deviate from stochiometric ratio, the system could be fully cured after proper curing thanks to the ability of CE to self-trimerization and the versatile epoxide ring opening chemistry. It is anticipated that those with higher CE concentrations will present the system with triazine components while the EP rich formulations will result in larger portion of polyether structures. The separation of the two curing exotherms was further investigated by the in-situ FTIR and the obtained spectra is shown in Fig. 2(b). When heated over the first exotherm, the consumption of cyanate groups (2250 cm^{-1}) and the appearance of triazine rings (1360 cm^{-1} and 1543 cm^{-1}) indicate the trimerization reaction of CE monomers [17,21,39], while no change of epoxide groups (915 cm^{-1}) [40] is noticed. At over 200 °C, the epoxide peak intensity gradually decreases with the oxazolidinone carbonyl groups (1747 cm^{-1}) [30] emerging. At the same time, the consumption of triazine groups is evidenced which is in accordance with the reaction route involving the insertion of epoxide on isocyanurate that reacts with other epoxide to give oxazolidinone structure. It can be concluded that the CE polymerization reaction takes place at lower temperature and the CE/EP copolymerization at high temperature. The chemical structure of the cured CE/ECN blends with different feed ratio is shown in Fig. 2(c). After curing, no signals form cyanate peaks (2250 cm^{-1}) or epoxide peaks (915 cm^{-1}) was found, indicating the high degree of conversion of these active functional groups. It is confirmed that the feed ratio of the two monomers did affect the chemical structures of the final cured copolymer. The triazine peak (1360 cm^{-1} and 1543 cm^{-1}) intensities increase with increasing CE concentrations and the oxazolidinone peak (1747 cm^{-1}) intensity follows the opposite trend, it is thus inferred that the triazine structures is more dominate in the CE rich formulations while the chain extending oxazolidinone groups constitute the major part of copolymers with low CE compositions.

3.1. Thermo-mechanical properties of the CE/ECN copolymers

As shown in TMA results from Table 2, increasing CE concentrations in the monomer feed results in a monotonic T_g increase of the samples. The 3:1 blend achieves a significantly improved T_g of approximately 250 °C compared to the 203.5 °C in the 1:3 blend. The CTE values of the copolymers both before and after the glass transition fall in the similar range as typical epoxy and their cyanate ester copolymers [31,41,42]. Considering the rubbery stage CTE (α_2), an initial decrease and then increase is noticed when increasing CE content, which implies the opposite trend of the polymer crosslink density.

The DMA tan δ profiles of the CE/ECN blends are shown in Fig. 4(a)

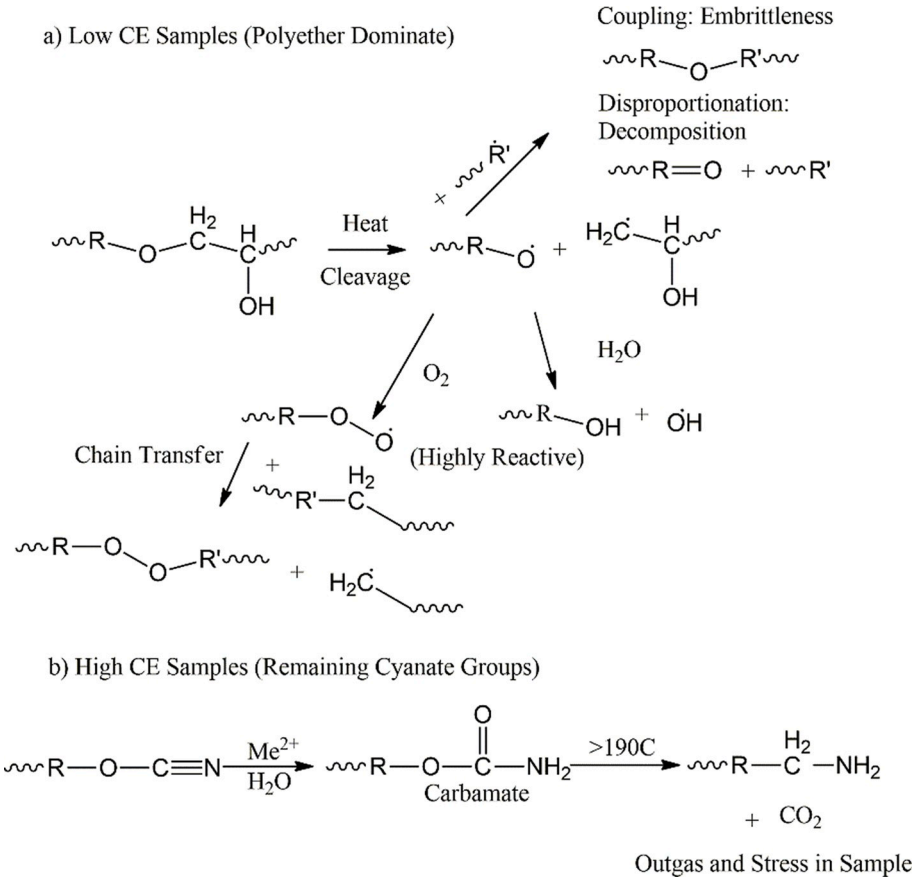

Fig. 8. Schemes of dominant degradation routes in the CE/ECN copolymer with different compositions. (a) low CE copolymer blends and (b) high CE copolymer blends.

and (b). In Fig. 4(a), the DMA T_g of the copolymer increases from 221.1 °C to 247.6 °C when the cyanate to epoxide ratios rise from 1:3 to 1:2. However, further increment in the CE feed does not lead to a notable change in T_g, apart from the extraordinarily high T_g of 291.1 °C in pure CE. Meanwhile, the area under tan δ curve which characterizes their damping properties are found to increase linearly with the CE proportion in the copolymer. Generally, the high damping factor would represent the characteristics of the loosely crosslinked polymers that tend to dissipate the applied energy. A more detailed look of the polymers ranging from 1:3 to 1:2 ratios is in Fig. 4(b). A continuous incremental T_g with shrinking damping factors when increasing the CE ratio is clearly evidenced. Based on the trend seen in the damping factor, it can be inferred that the crosslink density of the copolymer increases with a higher CE concentration in this range, which decreases when further increasing the CE feed ratio. One way to quantitatively estimate the crosslink density of a thermoset material is based on their storage modulus in the rubbery stage [43], whose formula is shown in equation (1).

$$Xc = \frac{G'}{3RT'} \tag{1}$$

where X_c is the estimated crosslink density, G′ is the storage modulus in the rubbery region (here at 30 °C higher than T_g), R is the ideal gas constant (R = 8.314 J/(mol·K)), T' = T_g + 30 °C. The properties calculated based on DMA data are listed in Table 3.

The crosslink density change is in the same trend as observed from α_2 and damping factor, and the order of magnitude of the obtained crosslink density is in good agreement with some reported values for cured thermosets including epoxies [44], polybenzoxazines [45] and polybenzoxazines with bisphenol additives [46]. The slightly higher value in this work might be related to the multifunctional nature of ECN and the high CE degree of conversion in the polymer blends. In the polymers with relative low CE contents, raising CE feed ratios concurrently increases the content of the rigid triazine structure and the crosslink density (due to a higher conversion of epoxides to oxazolidinone), thus promoting the T_g growth. However, further increase of the CE feed ratio will result in a reduced average functionality of the starting monomer and therefore the crosslink density of the cured copolymer, leading into the loosely crosslinked pure CE as an extreme. This fact balanced the effects of increased backbone rigidity due to further incorporation of triazine structures [36,47] and rendered the sample T_g remaining in the similar range for the formulations over 1:2 ratio.

The thermal decomposition profiles of the CE/ECN blends in N_2 are given in Fig. 4(c), and the weight loss derivative over temperature in Fig. 4(d). The parameters extracted from the TGA and DTG analysis are summarized in Table 4. Although poorer than the pure CE, the thermal stability of CE/ECN copolymers with different compositions exhibited interesting characteristics. From the magnified region in TGA and the DTG profile, when increasing CE concentration, the decomposition onset is pushed towards higher temperatures, while a large weight loss gradient is observed right after the initial decomposition that a lower decomposition peak temperature (T_p) is found. This phenomenon can also be explained by the competition between increasing triazine contents in the network and the decreasing matrix crosslink density/number of large aromatic molecules between ether linkages with higher CE concentration in the feed. In low CE contents polymers, although less triazine crosslinking nodes is present resulting in a lower decomposition onset, the further decomposition and loss of volatiles are affected by the physical structure in the resin. Their kinetics here is suppressed in these formulations due to not only the high crosslink density but also the

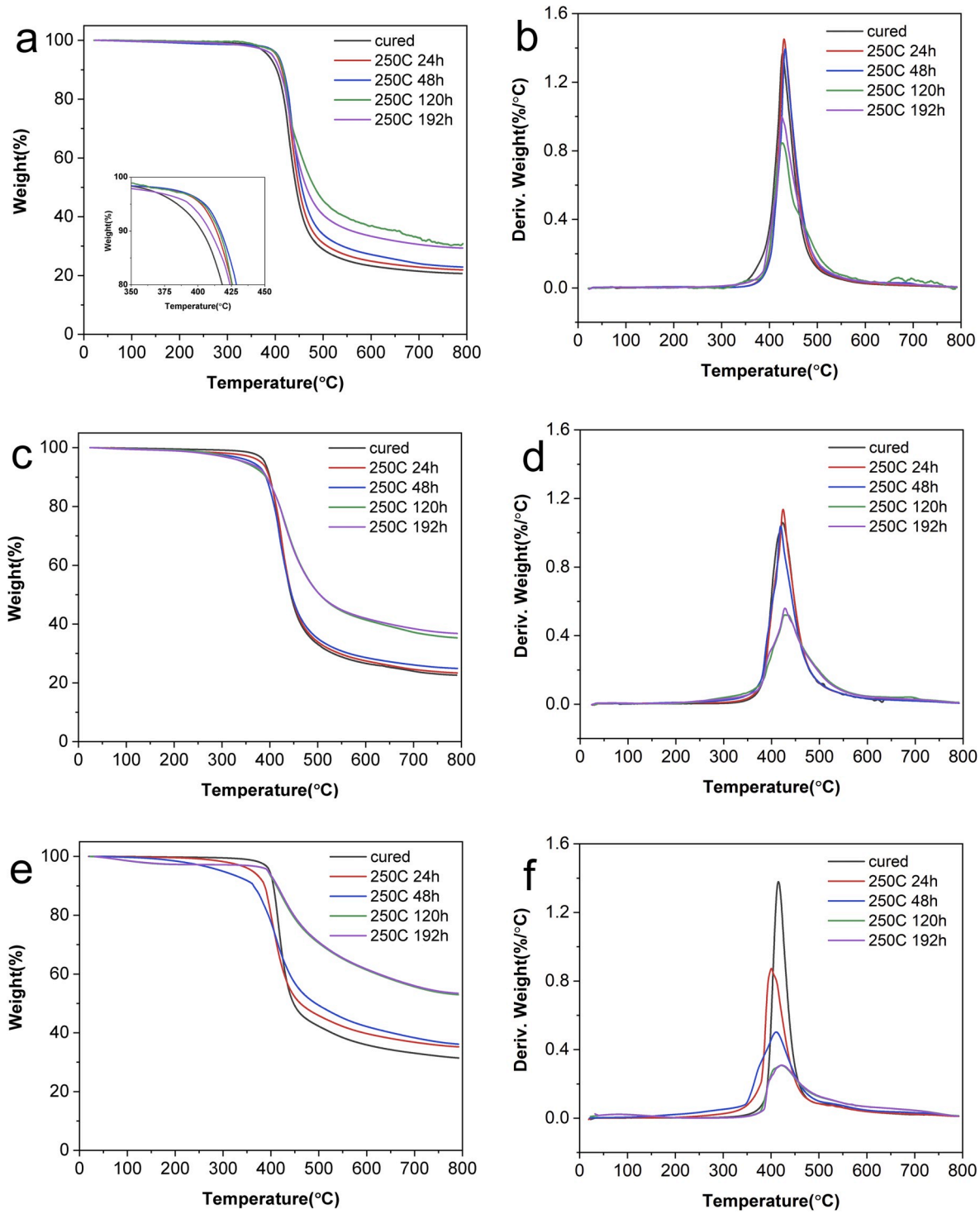

Fig. 9. TGA and DTG thermograms under N_2 of CE/ECN copolymers after different length of time under 250 °C aging. (a) and (b): CE/ECN 1:3 blend; (c) and (d): CE/ECN 1:1 blend; (e) and (f): CE/ECN 3:1 blend.

presence of abundant large aromatic building blocks between the weak ether linkages originated from ECN molecules. They are less likely to be broken or evaporated even after the initial decomposition. These features contributed to this unique behavior of the CE/ECN system on resisting the heat. From a technical point of view, the favorable thermo-mechanical properties in the CE/ECN blends with low CE concentrations suggest a promising future for their application as high temperature encapsulant materials.

The moisture absorption behavior of the polymer blends when subjected to 85 °C/85 RH condition is graphed in Fig. 5. Pure CE samples possess the highest moisture ingression rate and the equilibrium water content. Mixing the CE with ECN causes a reduced moisture absorption. Generally, the lower CE content polymers shows a lower water uptake, which is possibly due to the high crosslink density seen in these resins. It is also found that the dielectric constant of the copolymer decreases when increasing the CE concentration, as shown in Table 5. This should be related to the decrease of polarity in these polymers due to the lack of hydroxyl components that are introduced by epoxides.

Table 7
Summarized parameters from TGA and DTG thermogram of the CE/ECN blends after aging under 250 °C for different times.

CE/ECN	Aging time/h	$T_{5\%}$ in N_2/°C	$T_{10\%}$ in N_2/°C	Char Yield at 800 °C/%	T_p/°C
1:3	Cured	384.7	403.1	20.7	423.0
	24	401.7	413.9	21.9	430.5
	48	405.3	417.1	22.9	418.8
	120	403.5	415.9	30.6	428.0
	192	393.8	409.1	29.4	427.9
1:1	Cured	389.5	400.2	22.6	427.2
	24	380.7	398.8	23.4	424.0
	48	364.3	391.7	24.9	432.7
	120	347.2	392.1	35.3	426.1
	192	351.5	393.6	36.8	426.1
3:1	Cured	397.5	405.2	31.5	415.2
	24	360.	386.7	35.2	400.6
	48	299.4	364.0	36.2	410.2
	120	394.0	411.4	53.0	421.6
	192	393.8	413.5	53.4	422.8

3.2. High Temperature Aging Tests on CE/ECN Copolymers

Fig. 6(a) shows the results of high temperature storage test for the CE/ECN blends. Although the pure CE exhibits higher thermal stability in the initial 3–4 days, a large weight loss gradient emerged subsequently and associated with sample swelling and blistering that led to an early failure within 10 days. On the other hand, all the CE/ECN blends experienced a large initial decomposition rate but their weight loss in the longer term were retarded. Compared to the samples with lower CE contents, the higher CE formulations generally present larger weight losses during the high temperature aging in contrast to their better thermal stability in TGA studies. For example, the 3:1 CE/ECN sample holds a residue of only 40% after 1500 h. The appearance of the sample during the high temperature storage can be found in Fig. 6(b). Clearly the high CE content samples showed early shrinkage and warpage within 72 h, while the low CE polymers maintained their shapes until up to 300 h. Knowing the high T_g and high decomposition onset temperatures in the high CE polymers, it is to be further understood what made these polymers tend to fail and decompose drastically under high temperature aging condition.

TMA tests were carried out to illustrate the effects of high temperature storage on the thermomechanical properties of these resins. Table 6 summarizes these property changes during the aging test in first 48 h, where the formulation 1:3, 1:1 and 3:1 were selected to represent the nature of the material with different compositions. For the 1:3 sample, a first increased and then decreased T_g could be found during aging, while the α_2 followed an opposite trend. It has been known that further curing could take place when non-fully cured EP is exposed to elevated temperature for a prolonged time. In this case, it is likely that the EP dominated resin went through curing reaction to construct a higher crosslinked network during the first several hours of aging as evidenced by the T_g increase and α_2 drop. On the other hand, at temperature higher than T_g of the polymer, not only curing but thermal degradation could also be triggered since oxygen diffusion is greatly facilitated. The breakdown of network took place during the prolonged aging, resulting in the decrease in crosslink density and the T_g. Similar to the CE/ECN 1:3 polymer, the 1:1 formulation showed a slightly increased T_g after aging for 4 h. Further heating of the sample caused a monotonic T_g decrease and α_2 increase, which is the sign of chain scission and network breakdown. However, when increasing CE concentration to 3:1 ratio, the polymer properties exhibited a rather distinguished behavior during high temperature storage. Although the virgin 3:1 sample processed the highest T_g among all the samples, the dramatic and continuous T_g decrease was evidenced along the aging process. At the same time, the variation of α_2 was not in trend with aging time, which implies that the crosslink density change due to chain scission may not be appreciable.

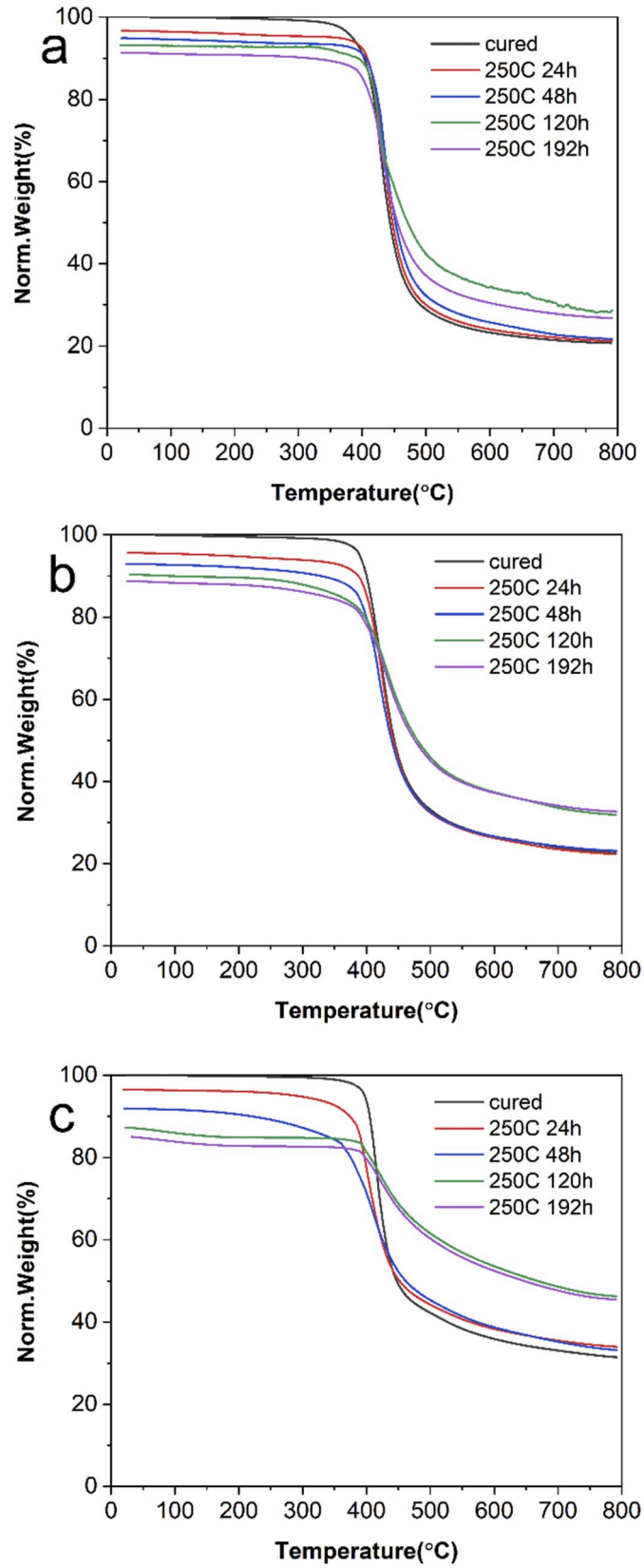

Fig. 10. Normalized TGA thermograms under N_2 of (a) CE/ECN 1:3 blend, (b) CE/ECN 1:1 blend and (c) CE/ECN 3:1 blend after different length of time under 250 °C aging using the aging weight loss data in Fig. 6(a).

Considering the high moisture absorption in this polymer and the sensitivity of CE to hydrolysis degradation, this behavior may be related to the plasticization effects of absorbed water and the outgas reactions from the formed carbamates.

The chemical structure change of these polymers during aging were monitored in order to gain insight into their degradation mechanism. The FTIR of CE/ECN 1:3, 1:1 and 3:1 polymer blends during aging could be found in Fig. 7(a), (b) and (c), respectively. From Fig. 7(a), one can first notice the gradual disappearance of epoxide absorption peaks at 915 cm^{-1} after 4 h which indicates the further curing of the EP rich polymers potentially with the hydroxyl or acid impurities in the resin at elevated temperature. As a result, the growth of the C–O stretching peak (broad peak around 1250 cm^{-1}) [48] is observed, as well as the O–H peaks (bending at around 1420 cm^{-1} and stretching at 3200 cm^{-1}) [49] due to epoxy ring opening. With further exposure to the high temperature, severe oxidative degradation may take place. The peak intensity of C═O groups (1660 cm^{-1} attributed to amide and 1740 cm^{-1} to ketone or aldehyde) [50] as well as that of the C–O and hydroxyl groups grow monotonically and drastically over time. It can be inferred that the degradation scheme of high EP content CE/ECN copolymer is dominated by the typical thermo-oxidative pattern seen in polyethers through the chain scission assisted by radicals reacting with oxygen [51,52], causing the decomposition of network structure (Fig. 8(a)). Similarly, the CE/ECN 1:1 copolymer exhibits the further consumption of epoxide groups during high temperature storage. However, the rise in hydroxyl group population was not obvious upon further aging. Still, the growth on C═O and C–O in the polymer indicates the presence of thermo-oxidation. Note that the rapid increase of intensity on C═O amide groups may also be attributed to the formation of carbamate groups from the CE hydrolysis. In the high CE content polymer, i.e. the CE/ECN 3:1 formulation, the main degradation mechanism is different from the low CE ones. In Fig. 7(c), the increasing carbonyl intensity can be clearly identified, and when correlating with the growing intensity of amine groups (N–H stretching at 3400 cm^{-1}) one can identify the formation of carbamate groups in the resin, which is in accordance with the analyses reported in various literatures [53–56]. The decomposition of the observed carbamates here can lead to the outgas and deformation of the resin physical network as seen in Fig. 8(b), which should be the main cause of the significant weight loss and T_g decrease in the high CE content polymers. This degradation route is believed to be able to generate localized thermal stress within the resin and finally lead to the mechanical failures such as sample warping and blistering.

The thermal decomposition behavior of the aged samples was also investigated. Fig. 9 shows the aging effects on the TGA and DTG properties of 1:3, 1:1 and 3:1 CE/ECN blends. The parameters extracted from TGA and DTG analysis are summarized in Table 7. In Fig. 9(a) inset and Fig. 9(b), an obvious higher decomposition onset is observed in all samples after aging conditions. In order to account for the weight loss that already occurred during aging, normalized weight diagrams are given in Fig. 10 according to the aging weight loss data shown in Fig. 6 (a). For CE/ECN 1:3 sample, a good matching of the weight loss profiles of unaged and aged samples could be found in the normalized plot Fig. 10(a), implying the similar degradation mechanism between the short-term thermal decomposition and the long-term aging degradation. For higher CE content formulations, the high temperature aging resulted in a very distinguished decomposition behavior compared to unaged sample. The normalized curve in Fig. 10 (b) showed a clear deviation of the aged CE/ECN 1:1 samples from its original decomposition curve, where a gradually decreasing onset temperature in longer aged samples was found (also see the T_p value from Table 7). It is thus inferred that other mechanisms rather than that in the short-term decomposition came into play when these samples are exposed to long-term high temperature aging conditions. As previously discussed in the FTIR studies, the induced stress from decomposition of carbamate groups in the high temperature aging conditions should be the main cause of these lowered decomposition onsets in aged samples. This phenomenon became even more obvious when further increasing the CE concentration in the resin, as shown in Fig. 9(e) and (f) as well as in Fig. 10(c). Much inferior thermal stability could be characterized in the lightly aged samples. For longer aged samples, e.g., the 120-h and the 192-h aged samples, they somehow exhibit a very similar weight loss pattern possibly because they are already in a charred stage lacking easily breakable chemical bonds. In conclusion, the greatly reduced T_g and thermal stability of high CE formulations samples are attributed to the unique degradation mechanism involving the hydrolysis degradations that can cause internal stress within the resin. This hydrolysis issue is to be emphasized and resolved if the high CE concentration CE/ECN blends are to be used in packaging applications for their high T_g or low K properties.

4. Conclusion

This paper provides a detailed evaluation of the high heat resistant CE/ECN copolymer blends for future high temperature electronic encapsulation applications. The characterizations on the thermo-mechanical properties of the copolymers as well as their long-term high temperature storage degradation are discussed with a specific focus on the resin composition effects. When altering the CE/ECN composition, the triazine content and crosslink density of the copolymers exhibit a tradeoff characteristic which affected their T_g and decomposition behavior. The low CE content formulations are able to produce high T_g and high heat resistant resins comparable to the high CE counterparts due to their high crosslink density and the plentiful stable aromatic molecule blocks between ether linkages. The high temperature (250 °C) storage causes significant weight loss and severe warpage and blistering in the high CE formulations. From the TMA, FTIR and TGA characterizations on the aged samples, it was found that the low CE polymers followed typical thermo-oxidative degradation patterns while the high CE formulations experienced a distinguished degradation route relates to the stress from the decomposition of carbamates after cyanate group hydrolysis. Overall, the 25 mol% to 33 mol% CE feed ratios are selected as the best formulation which are promising for future high temperature EMC studies while novel solutions against the hydrolysis degradation need to be posted for utilizing the dielectric properties in high CE content copolymers.

Declaration of competing interest

The authors declare that they have no known competing financial interests or personal relationships that could have appeared to influence the work reported in this paper.

CRediT authorship contribution statement

Jiaxiong Li: Conceptualization, Software, Investigation, Writing - original draft. **Chao Ren:** Data curation, Visualization. **Dong An:** Data curation, Writing - review & editing. **Yanjuan Ren:** Writing - review & editing. **Kyoung-sik Moon:** Methodology, Writing - review & editing. **Ching-ping Wong:** Supervision.

Acknowledgement

This work was supported by the Industry Consortium at the Georgia Tech Packaging Research Center (PRC).

References

[1] D. Lu, C. Wong, Materials for Advanced Packaging, Springer, 2009.
[2] N. Kinjo, M. Ogata, K. Nishi, A. Kaneda, K. Dušek, Epoxy Molding Compounds as Encapsulation Materials for Microelectronic Devices, Speciality Polymers/Polymer Physics, Springer, 1989, pp. 1–48.

[3] Y. Liu, Challenges of power electronic packaging, in: Y. Liu (Ed.), Power Electronic Packaging: Design, Assembly Process, Reliability and Modeling, Springer New York, New York, NY, 2012, pp. 1–8.
[4] G. Zhang, Z. Li, B. Zhang, W.A. Halang, Power electronics converters: past, present and future, Renew. Sustain. Energy Rev. 81 (2018) 2028–2044.
[5] A. Bindra, Wide-bandgap-based power devices: reshaping the power electronics landscape, IEEE Power Electronics Magazine 2 (1) (2015) 42–47.
[6] C. Chen, F. Luo, Y. Kang, A review of SiC power module packaging: layout, material system and integration, CPSS.Trans. Power Electron.Appl 2 (3) (2017) 170–186.
[7] Y. Yao, G.-Q. Lu, D. Boroyevich, K.D. Ngo, Survey of high-temperature polymeric encapsulants for power electronics packaging, IEEE Trans. Compon. Packag. Manuf. Technol. 5 (2) (2015) 168–181.
[8] A. Mavinkurve, L. Goumans, J. Martens, in: Epoxy Molding Compounds for High Temperature Applications, 2013 Eurpoean Microelectronics Packaging Conference (EMPC), IEEE, 2013, pp. 1–7.
[9] S. Levchik, A. Piotrowski, E. Weil, Q. Yao, New developments in flame retardancy of epoxy resins, Polym. Degrad. Stabil. 88 (1) (2005) 57–62.
[10] F.-L. Jin, X. Li, S.-J. Park, Synthesis and application of epoxy resins: a review, J. Ind. Eng. Chem. 29 (2015) 1–11.
[11] E. Nguegang, J. Franz, A. Kretschmann, H. Sandmaier, Aging effects of Epoxy Moulding Compound on the long-term stability of plastic package, in: 2010 11th International Thermal, Mechanical & Multi-Physics Simulation, and Experiments in Microelectronics and Microsystems (EuroSimE), IEEE, 2010, pp. 1–6.
[12] D. Leveque, A. Schieffer, A. Mavel, J.-F. Maire, Analysis of how thermal aging affects the long-term mechanical behavior and strength of polymer–matrix composites, Compos. Sci. Technol. 65 (3–4) (2005) 395–401.
[13] Y. Tanaka, I. Watanabe, in: Latest Developments of Molding Compound Material for Power Semiconductors, 2018 China Semiconductor Technology International Conference (CSTIC), IEEE, 2018, pp. 1–3.
[14] T. Agag, T. Takeichi, Synthesis and characterization of epoxy film cured with reactive polyimide, Polymer 40 (23) (1999) 6557–6563.
[15] R.J. Iredale, C. Ward, I. Hamerton, Modern advances in bismaleimide resin technology: a 21st century perspective on the chemistry of addition polyimides, Prog. Polym. Sci. 69 (2017) 1–21.
[16] C.P.R. Nair, D. Mathew, K.N. Ninan, Cyanate Ester Resins, Recent Developments, New Polymerization Techniques and Synthetic Methodologies, Springer Berlin Heidelberg, Berlin, Heidelberg, 2001, pp. 1–99.
[17] I. Hamerton, J.N. Hay, Recent developments in the chemistry of cyanate esters †, Polym. Int. 47 (4) (1998) 465–473.
[18] A. Tsiamis, R.J. Iredale, R. Backhouse, S.R. Hallett, I. Hamerton, Liquid processable, thermally stable, hydrophobic phenolic triazine resins for advanced composite applications, ACS Applied Polymer Materials 1 (6) (2019) 1458–1465.
[19] T.M. Keller, Phthalonitrile-based high temperature resin, J. Polym. Sci. Polym. Chem. 26 (12) (1988) 3199–3212.
[20] L.-S. Tan, F.E. Arnold, Benzocyclobutene in polymer synthesis. I. Homopolymerization of bisbenzocyclobutene aromatic imides to form high-temperature resistant thermosetting resins, J. Polym. Sci. Polym. Chem. 26 (7) (1988) 1819–1834.
[21] T. Fang, D.A. Shimp, Polycyanate esters: science and applications, Prog. Polym. Sci. 20 (1) (1995) 61–118.
[22] J. Li, C. Ren, K.-s. Moon, C.-p. Wong, Epoxy/Triazine Copolymer Resin System for High Temperature Encapsulant Applications, in: 2019 IEEE 69th Electronic Components and Technology Conference (ECTC), IEEE, 2019, pp. 2296–2301.
[23] M. Gaku, K. Suzuki, K. Nakamichi, Curable Resin Compositions of Cyanate Esters, Google Patents, 1978.
[24] D. Shimp, J. Christenson, S. Ising, Cyanate esters–an emerging family of versatile composite resins, in: Proceedings of the 34th Annual International SAMPE Symposium, 1989, pp. 222–233.
[25] J. Bauer, M. Bauer, Statistical structural model for the gelation behaviour of cyanate-epoxy polyreactions, Acta Polym. 39 (10) (1988) 548–551.
[26] M. Bauer, J. Bauer, Networks from cyanic acid esters and glycidyl ethers, Makromol. Chem., Macromol. Symp. 30 (1) (1989) 1–11.
[27] J. Bauer, M. Bauer, Kinetic structural model for the network build-up during the reaction of cyanic acid esters with glycidyl ethers, J. Macromol. Sci. Part A - Chemistry 27 (1) (1990) 97–116.
[28] I. Hamerton, J.N. Hay, Recent developments in the chemistry of cyanate esters, Polym. Int. 47 (4) (1998) 465–473.
[29] B.S. Kim, Effect of cyanate ester on the cure behavior and thermal stability of epoxy resin, J. Appl. Polym. Sci. 65 (1) (1997) 85–90.
[30] R.H. Lin, In situ FTIR and DSC investigation on cure reaction of liquid aromatic dicyanate ester with different types of epoxy resin, J. Polym. Sci. Polym. Chem. 38 (16) (2000) 2934–2944.
[31] W.F. Su, C.M. Chuang, Effects of chemical structure changes on curing reactions and thermal properties of cyanate ester-cured rigid-rod epoxy resins, J. Appl. Polym. Sci. 85 (11) (2002) 2419–2422.
[32] P. Ren, G. Liang, Z. Zhang, Epoxy-modified cyanate ester resin and its high-modulus carbon-fiber composites, Polym. Compos. 27 (4) (2006) 402–409.
[33] Y. Lei, M. Xu, M. Jiang, Y. Huang, X. Liu, Curing behaviors of cyanate ester/epoxy copolymers and their dielectric properties, High Perform. Polym. 29 (10) (2017) 1175–1184.
[34] S. Gouthaman, V. Madhu, S.O. Kanemoto, S.L. Madurai, I. Hamerton, Examining the thermal degradation behaviour of a series of cyanate ester homopolymers, Polym. Int. 68 (10) (2019) 1666–1672.
[35] M. Venkatesh, S. Gouthaman, S.O. Kanemoto, M.S. Lakshmi, I. Hamerton, Development of epoxy-cyanate ester-clay nanocomposites offering enhanced thermally stability, J. Appl. Polym. Sci. 136 (28) (2019) 47754.
[36] F. Wu, C.-C. Tuan, B. Song, K.-S. Moon, C.-P. Wong, Controlled synthesis and evaluation of cyanate ester/epoxy copolymer system for high temperature molding compounds, J. Polym. Sci. Polym. Chem. 56 (13) (2018) 1337–1345.
[37] M.R. Kessler, Cyanate Ester Resins Adapted from Cyanate Ester Resins, first ed., Wiley Encyclopedia of Composites, 2012, pp. 1–15.
[38] M. Bauer, J. Bauer, Aspects of the Kinetics, Modelling and Simulation of Network Build-Up during Cyanate Ester Cure, Chemistry and Technology of Cyanate Ester Resins, Springer, 1994, pp. 58–86.
[39] I. Hamerton, J.N. Hay, Recent technological developments in cyanate ester resins, High Perform. Polym. 10 (2) (1998) 163–174.
[40] M. Sánchez-Soto, P. Pagés, T. Lacorte, K. Briceño, F. Carrasco, Curing FTIR study and mechanical characterization of glass bead filled trifunctional epoxy composites, Compos. Sci. Technol. 67 (9) (2007) 1974–1985.
[41] T.-H. Ho, H.-J. Hwang, J.-Y. Shieh, M.-C. Chung, Thermal, physical and flame-retardant properties of phosphorus-containing epoxy cured with cyanate ester, React. Funct. Polym. 69 (3) (2009) 176–182.
[42] X. Zhang, A. Gu, G. Liang, D. Zhuo, L. Yuan, Liquid crystalline epoxy resin modified cyanate ester for high performance electronic packaging, J. Polym. Res. 18 (6) (2011) 1441–1450.
[43] I.M. Barszczewska-Rybarek, A. Korytkowska-Wałach, M. Kurcok, G. Chladek, J. Kasperski, DMA analysis of the structure of crosslinked poly (methyl methacrylate) s, Acta Bioeng. Biomech. 19 (1) (2017).
[44] S.B. Shen, H. Ishida, Dynamic mechanical and thermal characterization of high-performance polybenzoxazines, J. Polym. Sci. B Polym. Phys. 37 (23) (1999) 3257–3268.
[45] I. Hamerton, L.T. McNamara, B.J. Howlin, P.A. Smith, P. Cross, S. Ward, Examining the initiation of the polymerization mechanism and network development in aromatic polybenzoxazines, Macromolecules 46 (13) (2013) 5117–5132.
[46] W.A. Wan Hassan, J. Liu, B.J. Howlin, H. Ishida, I. Hamerton, Examining the influence of bisphenol A on the polymerisation and network properties of an aromatic benzoxazine, Polymer 88 (2016) 52–62.
[47] K. Dinakaran, M. Alagar, Preparation and characterization of epoxy-cyanate ester interpenetrating network matrices/organoclay nanocomposites, Polym. Adv. Technol. 14 (8) (2003) 574–585.
[48] A.G. Al Lafi, FTIR spectroscopic analysis of ion irradiated poly (ether ether ketone), Polym. Degrad. Stabil. 105 (2014) 122–133.
[49] P.R. Solomon, R.M. Carangelo, FTIR analaysis of coal. 1. Techniques and determination of hydroxyl concentrations, Fuel 61 (7) (1982) 663–669.
[50] B. Mailhot, S. Morlat, J.-L. Gardette, Photooxidation of blends of polystyrene and poly (vinyl methyl ether): FTIR and AFM studies, Polymer 41 (6) (2000) 1981–1988.
[51] N. Rose, M. Le Bras, S. Bourbigot, R. Delobel, Thermal oxidative degradation of epoxy resins: evaluation of their heat resistance using invariant kinetic parameters, Polym. Degrad. Stabil. 45 (3) (1994) 387–397.
[52] J. Pospíšil, Z. Horák, Z. Kruliš, S. Nešpůrek, S.-i. Kuroda, Degradation and aging of polymer blends I. Thermomechanical and thermal degradation, Polym. Degrad. Stabil. 65 (3) (1999) 405–414.
[53] J.T. Reams, A.J. Guenthner, K.R. Lamison, V. Vij, L.M. Lubin, J.M. Mabry, Effect of chemical structure and network formation on physical properties of di (cyanate ester) thermosets, ACS Appl. Mater. Interfaces 4 (2) (2012) 527–535.
[54] S.K. Karad, F.R. Jones, D. Attwood, Moisture absorption by cyanate ester modified epoxy resin matrices. Part I. Effect of spiking parameters, Polymer 43 (19) (2002) 5209–5218.
[55] E. Kollia, T. Loutas, E. Fiamegkou, A. Vavouliotis, V. Kostopoulos, Degradation behavior of glass fiber reinforced cyanate ester composites under hydrothermal ageing, Polym. Degrad. Stabil. 121 (2015) 200–207.
[56] A.O. Crawford, G. Cavalli, B.J. Howlin, I. Hamerton, Improving the hydrolytic stability of aryl cyanate esters by examining the effects of extreme environments on polycyanurate copolymers, React. Funct. Polym. 109 (2016) 104–111.